Engineering and Applied Science Letters

PSR Press

Article

Comparison of the anisotropic and isotropic macroscopic traffic flow models

Gabriel Obed Fosu[1,*], Gideon K. Gogovi[2] and Joshua K. Asamoah[1]

[1] Department of Mathematics, Kwame Nkrumah University of Science and Technology, Ghana.
[2] Department of Mathematics and Statistics, University of Houston-Downtown, Houston, USA.
* Correspondence: gabriel.of@knust.edu.gh

Received: 20 April 2023; Accepted: 5 May 2023; Published: 30 June 2023.

Abstract: Second-order macroscopic vehicular traffic flow models are categorized under two broad headings based on the direction of their characteristics. Faster-than-vehicle waves are often called isotropic models vis-á-vis anisotropic models with slower-than-vehicle characteristic speed. The dispute on the supremacy among these families of models is the motivation for this paper. This paper compares and contrasts six distinctive second-order macroscopic models using a numerical simulation and analysis. Three models are characterized by faster-than-vehicle waves with their corresponding anisotropic counterparts. Simulation results on the formation of deceleration waves and the dissolution of acceleration fans are presented to graphically compare the wave profiles of the selected isotropic and anisotropic traffic models. Observably, these opposing models can all characterize these physical traffic phenomena to the same degree. Thus, faster characteristic speed conceptualization of second-order macroscopic equations does not tantamount to model failure but rather lies in the explanation of this property.

Keywords: Characteristic speed; multilane flow; traffic waves; isotropic models; anisotropic models.

1. Introduction

A hypothetical description of the relationship among drivers-vehicles has been a concern to both engineers and physicists [1–3]. To demystify this complex phenomenon several microscopic and macroscopic models have been developed [4–11]. Microscopic models explain the interaction among individual drivers and vehicles. In contrast, at the macroscopic level, the collective behavior of drivers-vehicles is considered. A few research works [12,13] are known to be the inaugural offshoot of macroscopic equations. The equation has been titled using the author's initials, referred to as the Lighthill-Whitham-Richards (LWR model). They derived an elementary flow model from the conservation principle. As simple as their formulation was, the LWR model makes plain and comprehensible certain linear and non-linear physical processes governing traffic flow.

The drawbacks of this first-order equation brought forth into existence higher order models [14–18]. Payne[14] and Whitham [15] introduced the speed evolution equation to make up for the defect of infinite acceleration by the LWR. The momentum equation was derived from the microscopic car-following model. The constituents of this equation include convection, anticipation, and relaxation. The convective part ensures that the velocities toward a given source and away from the source fall into perspective. Relaxation captures how drivers-vehicles would adjust their velocities to the optimal velocity. The convection and the relaxation components are the same amidst all second-order models. The varied representation of traffic anticipation has led to divergent second-order models. Different expressions have been used to describe how drivers perceive and react to frontal traffic conditions. The isotropy and anisotropy feature of traffic flow depends on the orientation of the anticipation or pressure term. Isotropy is used here to denote a class of models that have characteristic speed faster than vehicle speed. On the other hand, anisotropy makes reference models which have vehicles' velocity traveling faster than all the characteristics.

The Payne-Whitham-like (PW) models have two propagation speed values. One of these often travels faster than the velocity of the traffic. That is to say, vehicles react to information from behind. This accounts for the isotropic property of all PW models. In an earlier publication, Helbing and Johansson [19] asserted

that the faster-that-traffic characteristic does not constitute model inconsistency as opposed to a contrary view by some other researchers [20,21]. The authors [19] juxtaposed the PW model with the optimal velocity (OV) model and concluded that both models exhibit the same wave propagation characteristics. The phase and group velocities were obtained to be the same for both the macroscopic PW model and the microscopic OV model. For these authors, the property of a backward traveling wave should not be linked to the interaction among vehicles but rather the acceleration process of drivers.

In the past, some authors considered the backward traveling wave property as a flaw and proposed models having anisotropic features. Though there are several models exhibiting non-faster-than-vehicles property [22–25], the conceptualization by [26] is opted as the classical case. The abbreviation JWZ (Jiang-Wu-Zhu) will be used interchangeably with this classical model. As a new postulation, [26] replaced the density-dependent pressure term with a velocity-dependent component. The JWZ model is known to have all characteristic either equal or less than the vehicles speed. All other ensuing models mimicking this velocity-gradient anticipation are anisotropic [10,27]. Here, trailing information does not influence driving behaviour.

To date, the option of the most suitable second-order isotropic/anisotropic macroscopic model still lingers in the minds of transportation engineers. In a back and forth babble [19,28,29] the authors recommended computational simulations further to settle the mist between faster-than-vehicles and non-faster-than-vehicles models. This paper aims to have a concord among these models by employing a numerical simulation comparison. A series of real traffic scenarios are presented graphically to examine the similarities or differences among these opposing families of models. The models considered are the classical PW model, classical JWZ model, viscous PW model, viscous JWZ model, viscous-diffusive PW model, and viscous-diffusive JWZ model. Each isotropic model has its anisotropic twin.

The remaining portion of the paper is organized as follows. In the next section, the model equations together with the instability conditions are presented. A graphical analysis of queue formation and jam dissolution follows this. In addition, the continuum models are expressed in their discrete forms to visualize their similitude within the framework of multilane traffic. In the final section, we present summarized conclusions from the study.

2. The Models

Second-order models are expressed mathematically by a system of partial differential equations: a continuity equation and a dynamic velocity equation. In this research, the construct of the continuity equation remains the same for both isotropic and anisotropic families of models. Nonetheless, the acceleration equations are different. The choice of the pressure gradient term accounts for these differences. That is either a density-dependent gradient or a velocity-dependent gradient. For the classical PW, viscous PW, and viscous-diffusive PW models, driver anticipation is based on the density ahead. Their anisotropic pairs, classical JWZ, viscous JWZ, and the viscous-diffusive JWZ have a velocity-dependent anticipation term.

2.1. Classical Continuum Models

The two classical models are the isotropic PW model and the anisotropic JWZ model. The PW model is expressed as

$$k_t + (ku)_x = 0, \tag{1}$$

$$u_t + uu_x = \frac{U(k) - u}{\tau} - \frac{c^2(k)}{k} k_x, \tag{2}$$

k is the density and u is the traffic speed, $c(k)$ is analogous to the sonic speed. $U(k)$ is the optimal speed depending entirely on density; the relaxation time τ determines how quickly traffic reinstates itself to steady-state conditions. The expression containing τ accounts for traffic relaxation. The last term of equation (2) is the anticipation term. It delineates the responsiveness of drivers to adapt to onward traffic information.

This classical model has two eigenvalues (characteristic speed);

$$\Lambda_1 = u - c(k),\ \Lambda_2 = u + c(k). \tag{3}$$

The speed of the latter $u + c(k)$ is well-known to be faster than the speed of the traffic u. This accounts for the isotropic feature of the PW model. Drivers' reaction to information is invariant concerning direction.

Again, the contrariwise transition from stable to unstable traffic regimes is explained by the inequality [10]

$$\left|\frac{dU(k_e)}{dk}\right| k_e^2 \leq \frac{1}{2\tau}, \tag{4}$$

k_e is the uniform density. Traffic will break down when the value on the left-hand side of the inequality (4) exceeds the value of the right. This could occur when the resulting value of a change in velocity due to changes in traffic density is significantly large. This is associated with traffic that has a moderate flow rate. Alternatively, a shorter reaction time could also cause the flow to collapse.

The classical JWZ replaces the density-dependent in the momentum equation with a velocity-dependent slope. The authors also replaced the density-dependent sound speed $c(k)$ with the constant c_k. The equation of motion is recast as:

$$u_t + uu_x = \frac{U(k) - u}{\tau} + c_k u_x. \tag{5}$$

The second-order JWZ model (1) and (5) also has two characteristic speed values. They are as follows

$$\Lambda_1 = u - c(k),\ \Lambda_2 = u. \tag{6}$$

Both eigenvalues do not exceed the vehicle's speed. The propagation of the characteristics is unilateral. This explains why drivers respond to only frontal information in anisotropic modeling.

Through a similar linear stability analysis used to obtain (4), the stability condition for the classical JWZ model is given as:

$$\left|\frac{dU(k_e)}{dk}\right| k_e \leq c_k. \tag{7}$$

We would observe a stop-and-start flow with a greater than inequality. As a comparison, the equilibrium conditions (4) and (7) are equivalent when $c_k = 1/2\tau k_e$. This demonstrates a similitude between the isotropic model and its anisotropic counterpart.

2.2. Viscous Continuum Models

The classical PW model has been improved to give a more accurate picture of real traffic [16,18,30,31]. Most recently the speed evolution equation was modified to capture velocity differences across multiple lane flow [10]. The PW was extended from a single spatial domain to two spatial domains to incorporate some lateral effect on multilane flow. An additional viscous term is introduced to capture some transverse occurrences. The new source term comprises viscosity rate, velocity differential, and an inter-lane sensitivity parameter. The sensitivity follows a similar analogy of microscopic modeling [32,33]. One peculiar assumption made was that the vehicle's speed on a multilane highway varied from one lane to the other. This add-on was founded on the principle of increasing/decreasing speed/density moving from the outer lanes to the inner lanes. For example, on most highways or roads with more than one lane, the outer lane is usually used by lower-speeding vehicles; hence, drivers trolling along the outer lanes have lower speeds than vehicles in the inner lanes. This is connected with a near stop traffic on the extreme outer lane. Hither, the viscous term is appended to the PW and the JWZ models hereinafter referred to as the viscous PW model and the viscous JWZ model respectively. The viscous isotropic model is of the form:

$$\begin{aligned} k_t + (ku)_x &= 0, \\ u_t + uu_x &= \frac{U(k) - u}{\tau} - \frac{1}{k}\left[c^2(k)k_x, +\mu\zeta u_y\right], \end{aligned} \tag{8}$$

ζ and μ are respectively the sensitivity and viscosity parameters. The anisotropic correspondence is also of the form:

$$u_t + uu_x = \frac{U(k) - u}{\tau} + c_k u_x - \frac{\mu\zeta}{k} u_y, \tag{9}$$

Note that the LWR equation remains the same as earlier.

The characteristics of these viscous models are not different from their initial forms. The classical models and their viscous counterparts have the same homogeneous parts.

The steady state solution for the viscous isotropic model is given by the expression:

$$\left|\frac{dU(k_e)}{dk}\right| k_e^2 \leq \frac{1}{2\tau} - \mu\zeta\frac{s_2}{s_1}, \tag{10}$$

$s_{1,2}$ are the spatial wavelength notations adapted for the linear stability computations. s_1 models the longitudinal wavelength and the lateral being represented by s_2. If the ratio of these wavelengths equal unity, then (10) reduces to

$$\left[\frac{dU(k_e)}{dk}\right] k_e^2 \leq \frac{1}{2\tau} - \mu\zeta. \tag{11}$$

Juxtaposing equation (4) side by side with (11), we take cognizance of an additional term $\mu\zeta$. Indicating that this viscous quantities (viscosity and sensitivity) play significant role in determining steady flow. Since the quantum of these parameters are non-negative, then value of $1/2\tau - \mu\zeta$ becomes more diminutive. Therefore, traffic should be more dense or lighter to achieve a continuous uniform flow.

By similar computation we obtain

$$\left|\frac{dU(k_e)}{dk}\right| k_e^2 \leq c_k k_e - \mu\zeta, \tag{12}$$

as the steady state solution for the viscous anisotropic model. The term $\mu\zeta$ resurfaces in the steady state solution of this viscous model. Again, portraying a close relation between faster-than-vehicles models and non-faster-than-vehicles models.

2.3. Viscous-Diffusive Continuum Models

These are the last category of models considered. Let's first clarify the use of these captioned terms. In the past, models with the second-order derivative term concerning space were classified as viscous models [16,17,27]. But in 2022, [10] added to the literature by distinguishing between viscosity along the traffic and viscosity across the flow; they emphasized that the predecessors generalized longitudinal viscosity for traffic resistance. The physics of this conceptualization is accounted for by diffusion. For brevity, the second-order derivative terms are captioned as diffusion because of their similitude with the diffusion equation. Traffic engineers modeled the diffusion term to smooth shocks across different traffic regimes, while lateral resistance was named viscosity.

Furthermore, we modify these viscous equations by adding to it the diffusion term. The mathematical formalism of their momentum equations is as follows:

Viscous-diffusive isotropic model

$$u_t + uu_x = \frac{U(k) - u}{\tau} - \frac{1}{k}\left[c^2(k)k_x + \mu\zeta u_y\right] + Du_{xx}. \tag{13}$$

Viscous-diffusive anisotropic model

$$u_t + uu_x = \frac{U(k) - u}{\tau} + c_k u_x - \frac{\mu\zeta}{k}u_y + Du_{xx}.$$

Simplified as

$$u_t = (c_k - u)u_x + \frac{U(k) - u}{\tau} - \frac{\mu\zeta}{k}u_y + Du_{xx}. \tag{14}$$

We again notice that the homogeneous part has still not changed. Hence, the viscous-diffusive models have the same characteristic speed values as their pairs discussed earlier. Some others are of the view that isotropic characteristics violate causality [20,25], and others have proven that they are all consistent with theoretical facts [34,35]. In the next section, we continue with some computational simulations as our contribution to elucidating this controversy.

3. Numerical Simulation of The Continuum Models

This analysis is focused primarily on the viscous-diffusive models since the other models (classical and viscous PW/JWZ) form a limiting case of these modified models.

3.1. Numerical Scheme

Before the graphical results are presented, it is worthwhile to discuss the numerical discretization scheme employed. These continuous partial differential equations are expressed as discrete difference equation because mathematical simulation software are often programmed to accept discrete inputs. These model equations (1) and (13) are discretized using the finite difference scheme. The continuity equation $k_t = -ku_x - uk_x$ is discretized as [26,27]:

$$k_i(j+1) = k_i(j) - \Delta t k_i(j)\frac{(u_{i+1}(j) - u_i(j))}{\Delta x} - \Delta t u_i(j)\frac{(k_i(j) - k_{i-1}(j))}{\Delta x}. \tag{15}$$

Also, the viscous-diffusive isotropic acceleration equation is expressed as [36,37]:

$$u_i(j+1) = u_i(j) - \Delta t u_i(j)\frac{(u_i(j) - u_{i-1}(j))}{\Delta x} + \frac{\Delta t}{\tau}(U(k_i(j)) - u_i(j)) - \frac{\Delta t}{k_i(j)+\chi}\left[c^2(k)\frac{k_{i+1}(j) - k_i(j)}{\Delta x} + \mu\zeta\frac{u_i^l(j) - u_i^{l-1}(j)}{\Delta y}\right] + D\Delta t\frac{(u_{i+1}(j) - 2u_i(j) + u_{i-1}(j))}{(\Delta x)^2}. \tag{16}$$

The sound speed is assumed to be constant and χ is introduced to model the deficiency of a zero-density value.

The partial differential equation (14) has two discrete equations. One of these equations exemplifies light traffic when the vehicle speed exceeds the sonic speed. The other discrete equation illustrates the case of heavy traffic when the sonic speed travels faster than the speed of vehicles [26,27]. The details are presented in equations (17) and (18) below:
Congested flow equation:

$$u_i(j+1) = u_i(j) + \Delta t(c_k - u_i(j))\frac{(u_{i+1}(j) - u_i(j))}{\Delta x} + \frac{\Delta t}{\tau}(U(k_i(j)) - u_i(j)) - \frac{\mu\zeta\Delta t}{k_i(j)+\chi}\cdot\frac{u_i^l(j) - u_i^{l-1}(j)}{\Delta y} + D\Delta t\frac{(u_{i+1}(j) - 2u_i(j) + u_{i-1}(j))}{(\Delta x)^2}. \tag{17}$$

Free flow equation:

$$u_i(j+1) = u_i(j) + \Delta t(c_k - u_i(j))\frac{(u_i(j) - u_{i-1}(j))}{\Delta x} + \frac{\Delta t}{\tau}(U(k_i(j)) - u_i(j)) - \frac{\mu\zeta\Delta t}{k_i(j)+\chi}\cdot\frac{u_i^l(j) - u_i^{l-1}(j)}{\Delta y} + D\Delta t\frac{(u_{i+1}(j) - 2u_i(j) + u_{i-1}(j))}{(\Delta x)^2}, \tag{18}$$

where $i = 1, \cdots, I$; $j = 0, \cdots, J-1$; and $l = 1, \cdots L$. The temporal period is divided into j units with step size Δt. There are L number of lanes. For this single-piped analysis, the velocity differential for any two adjacent lanes is also assumed to be constant. Hence $u_i^l(j) - u_i^{l-1}(j)$ is replaced with a constant value u_y. The fundamental equation proposed by [38] is adopted to complete the requirement of $U(k)$.

$$U(k_i(j)) = u_{max} - u_{max} * exp\left[1 - exp\left(\frac{k_w}{u_{max}}\left(\frac{k_{max}}{k_i(j)}\right) - 1\right)\right]. \tag{19}$$

3.2. Simulation Setup

The following initial conditions are used to simulate and compare acceleration and deceleration waves.

Declaration wave: Acceleration wave:

$$k(x,0) = \begin{cases} 0.775veh/m, & \text{for } x \leq \alpha, \\ 1.000veh/m, & \text{for } x > \alpha, \end{cases} \qquad k(x,0) = \begin{cases} 1.000veh/m, & \text{for } x \leq \alpha, \\ 0.150veh/m, & \text{for } x > \alpha. \end{cases}$$

Assuming a $10km$ stretch, then the discontinuity is located at $x = \alpha = 5km$. The specifics of these parameters are explained in Table 1.

Table 1. Parameter setup for simulation

Name	Notation	Value
Speed differentials	u_y	5.55m/s
Viscosity rate	μ	0.00141
Diffusion rate	D	10.00
Sensitivity rate	ζ	0.37
Maximum density	k_{max}	$1.00veh/m$
Maximum speed	u_{max}	$20.00m/s$
Kinematic speed	k_w	$11.00m/s$
Sonic speeds	$c(k)$	$5.00m/s$
	c_k	$3.00m/s$
Step sizes	Δx	$100.00m$
	Δy	$1.00m$
	Δt	$1.00s$
Relaxation time	τ	$10.00s$
Artificial density	χ	$0.33veh/s$

The boundaries follow the initial density profiles at the extrema. A ten-minute experimental results are presented in the next section.

3.3. Simulation Results

This continuum analysis is performed to compare how this family of models is able to capture the traffic dynamics of queue formation and its dissolution. The question asked is, are both model classifications able to conceptualize these physical realities? The results of these simulations are shown in the figures below. In all cases, we compare the faster-than-vehicles to the non-faster-than-vehicles models by examining how density and speed evolve over time.

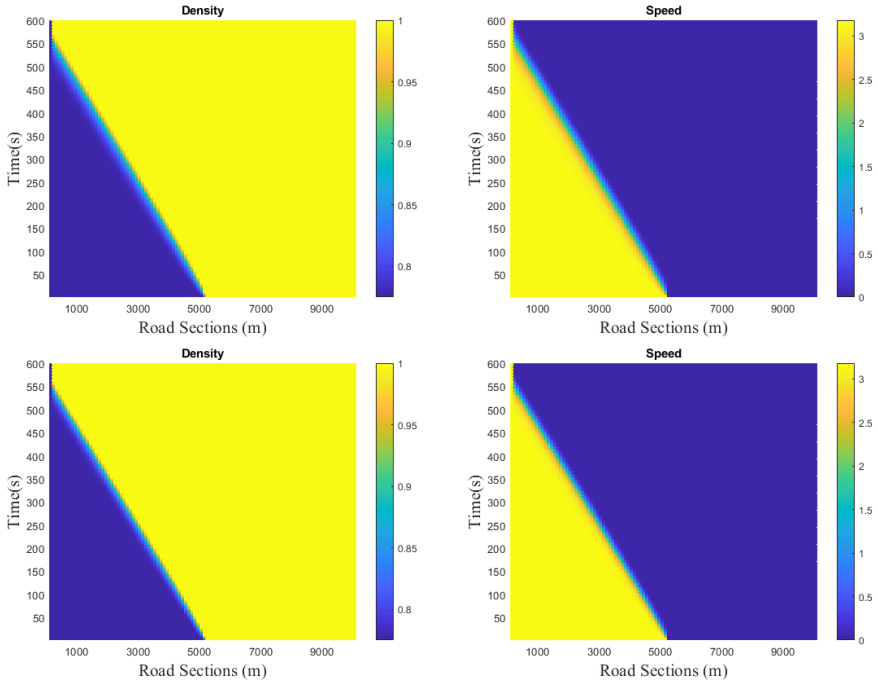

Figure 1. Deceleration wave profiles using the viscous-diffusive isotropic model (top) and anisotropic model (bottom)

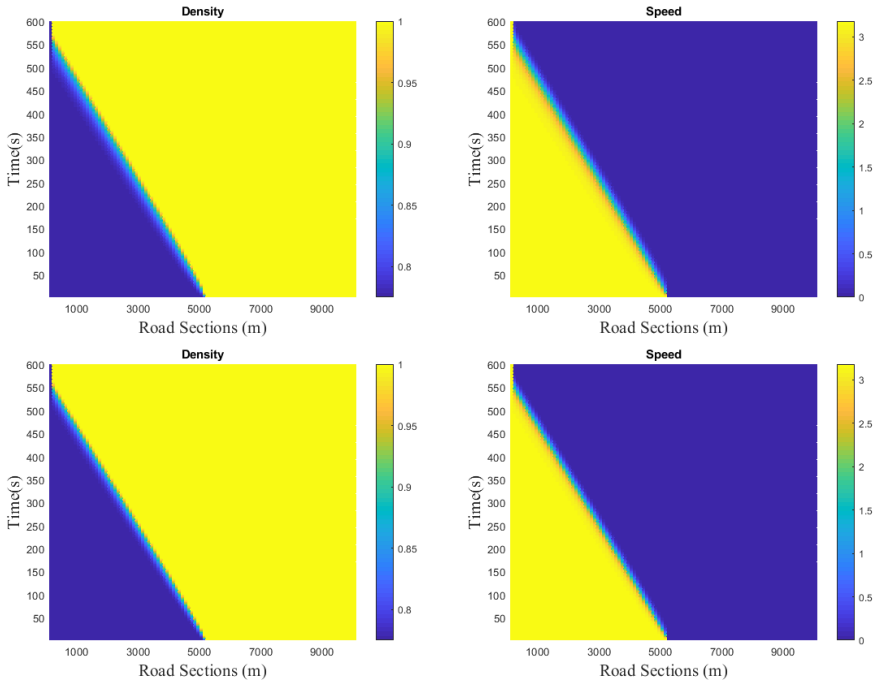

Figure 2. Deceleration wave profiles using the viscous isotropic model (top) and anisotropic model (bottom)

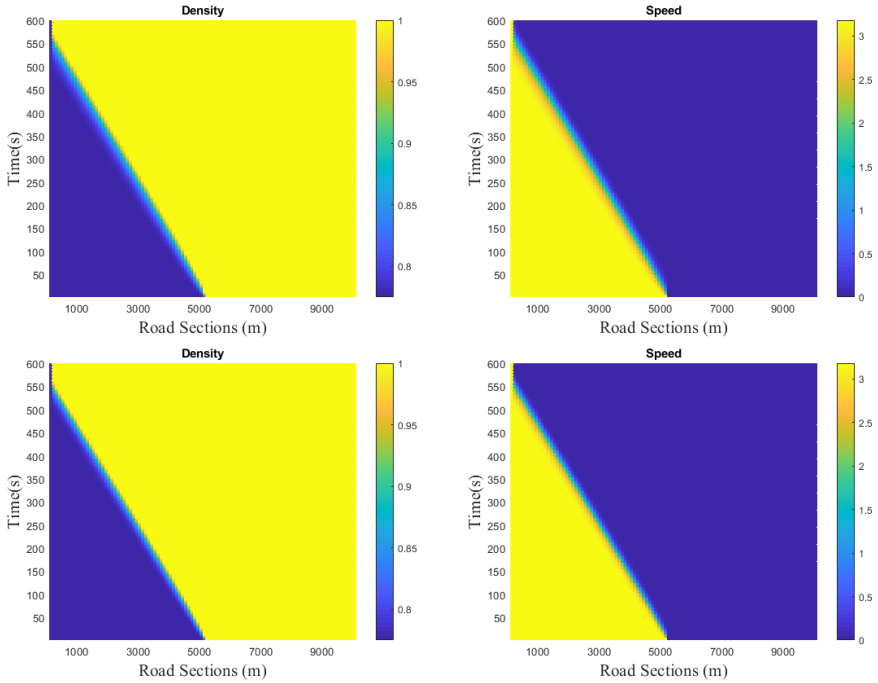

Figure 3. Deceleration wave profiles using the classical isotropic model (top) and anisotropic model (bottom)

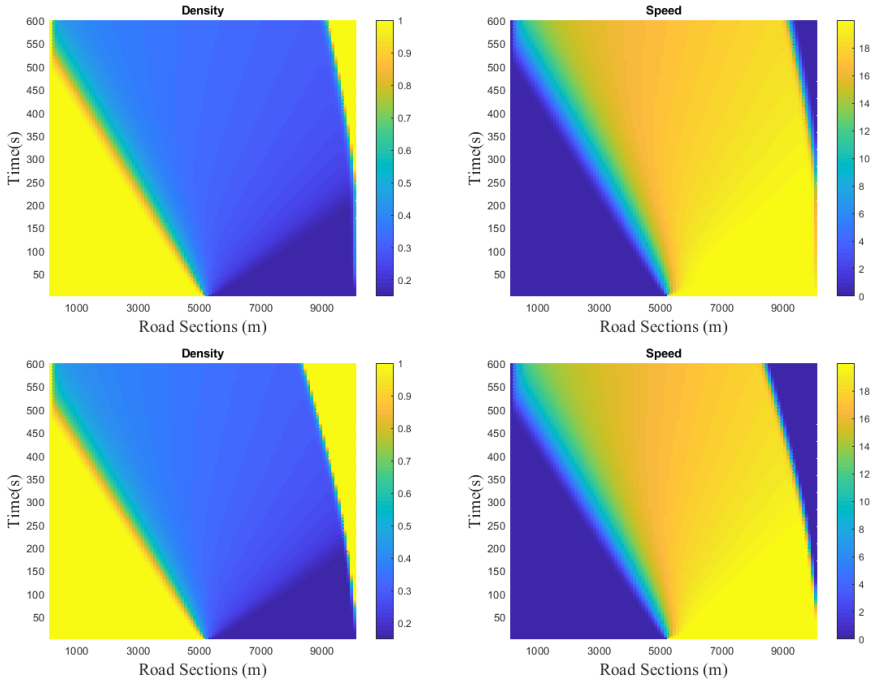

Figure 4. Acceleration wave profiles using the viscous-diffusive isotropic model (top) and anisotropic model (bottom)

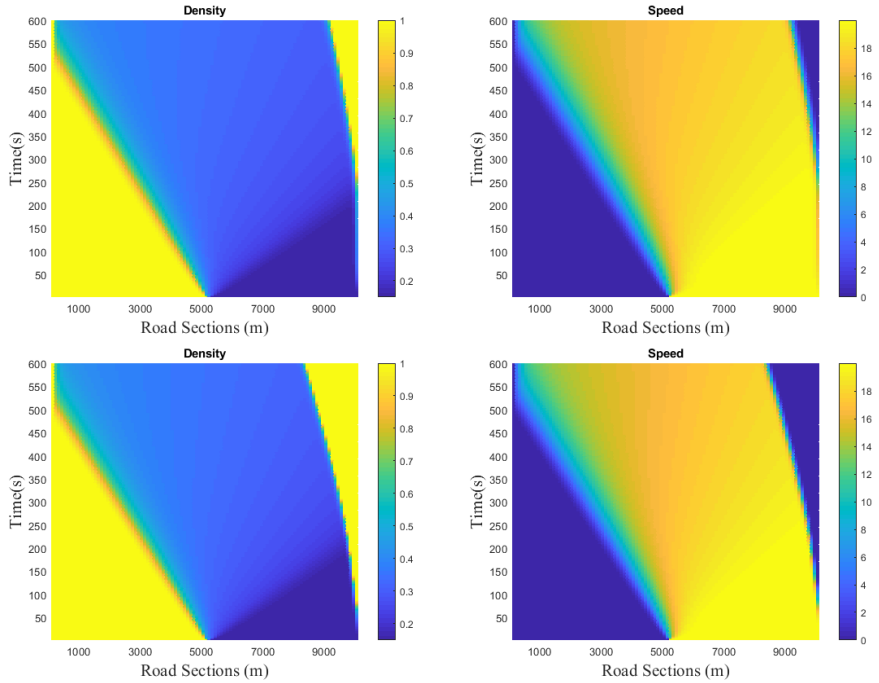

Figure 5. Acceleration wave profiles using the viscous isotropic model (top) and anisotropic model (bottom)

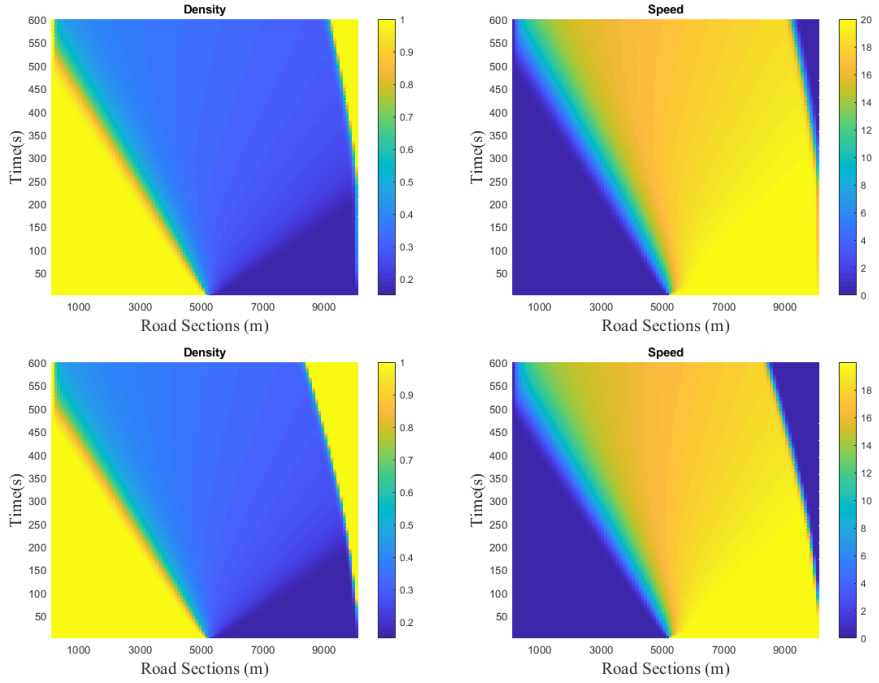

Figure 6. Shock wave profiles using the classical isotropic model (top) and anisotropic model (bottom)

Figures 1 and 2 are respectively the deceleration and acceleration traffic waves resulting from the viscous-diffusive models. The plots of the isotropic models are in similitude with the anisotropic models. The pair above correspond to the faster-than-vehicles models, while non-faster-than-vehicles models are placed exactly beneath them. Moreover, we run a series of tests using the viscous models (Figures 2 and 5) and the classical equations (Figures 3 and 6) to probe whether the controversy among these models is worth it or just an illusion. These simulations do give enough room to argue that anisotropic traffic models are not superior to their isotropic counterparts. They are all equally able to capture this dynamic traffic phenomenon. These models provide accurate predictions of real traffic. From Figures 1-3, we observe a backward traveling wave as a result of the jam density ahead. Since traffic has come to a complete halt, vehicles far upstream will be

required to align their speed to the optimal congested concentration values. For the acceleration fans (Figures 4-6), there is a continual dissolution of the queues because of a lighter downstream density. However, the queue begins to form again at the end of the road. This illustrates that vehicles with moving towards another dense traffic, such as driving through two cities. On the contrary, the differences between the classical, viscous, and viscous-diffusive plots are not clearly perceptible.

4. Conclusion

In this paper, we present a comparative study of anisotropic and isotropic traffic models. Isotropic models are characterized by the driver's reaction to both forward and backward stimuli as opposed to anisotropic models where drivers respond to only frontal information. Three isotropic models were compared with their anisotropic pairs to reconcile the rivalry between these families of models. These comparisons were demonstrated with conditions for steady-state flow, graphical simulation of their acceleration fans, and their deceleration wave profiles. Each pair was elicited from the classical second-order models, the viscous macroscopic flow models, and the viscous-diffusive continuum traffic models.

On reviewing the traffic instability, it was observed that the conditions of determining a stable flow using the faster-that-traffic models had some level of equivalence to non-faster-than-traffic models. The premise for total equality was observed when the value of the sonic speed c_k was equal to $1/2\tau k_e$; where τ is the relation time and k_e is the steady state density.

Moreover, simulations were performed to examine the similarities and or differences among these selected models with visualizations. A non-linear dynamic phenomenon that is of much concern for traffic engineers was selected for these comparisons; that is contraction and expansion traffic wave profiles. The speed and density profiles on shocks and rarefaction using the Payne-Whitham models are compared with Jiang-Wu-Zhu models. Characteristically, we observed no distinct differences between these rivalry models. The wave formation and dissolution of these models had very similar resemblances within the spatial and temporal simulation space. Though these classes of models presented had different mathematical representations, they all explain these non-linear features. Either anisotropic or isotropic they produce equivalent characterization of realistic vehicular traffic flow.

Author Contributions: All authors contributed equally to the writing of this paper. All authors read and approved the final manuscript.

Conflicts of Interest: The authors declare no conflict of interest.

References

[1] Helbing, D. (2001). Traffic and related self-driven many-particle systems. *Reviews of Modern Physics, 73*(4), 1067.

[2] Herty, M., Fazekas, A., & Visconti, G. (2017). A two-dimensional data-driven model for traffic flow on highways. *arXiv preprint arXiv:1706.07965*.

[3] Herty, M., Moutari, S., & Visconti, G. (2018). Macroscopic modeling of multi-lane motorways using a two-dimensional second-order model of traffic flow. *SIAM Journal on Applied Mathematics, 78*(4), 2252-2278.

[4] Newell, G.F. (2002). A simplified car-following theory: a lower order model. *Transportation Research Part B: Methodological, 36*(3), 195-205.

[5] Bogdanova, A., Smirnova, M. N., Zhu, Z., & Smirnov, N. N. (2015). Exploring peculiarities of traffic flows with a viscoelastic model. *Transportmetrica A: Transport Science, 11*(7), 561-578.

[6] Chavan, R., Mulla, A.K., Chakraborty, D., & Manjunath, D. (2016). A model for lane-less traffic with local control laws. In *European Control Conference: IEEE* (Vol. 1, pp. 2447-2452).

[7] Khan, Z. H., & Gulliver, T. A. (2018). A macroscopic traffic model for traffic flow harmonization. *European Transport Research Review, 10*(2), 1-12.

[8] Wang, T., Zhao, J., & Li, P. (2018). An extended car-following model at un-signalized intersections under V2V communication environment. *PloS one, 13*(2), e0192787.

[9] van Beinum, A., Hovenga, M., Knoop, V., Farah, H., Wegman, F., & Hoogendoorn, S. (2018). Macroscopic traffic flow changes around ramps. Transportmetrica A: Transport Science, 14(7), 598-614.

[10] Fosu, G.O., Adu-Sackey, A., & Ackora-Prah, J. (2020). Macroscopic analysis of the viscous-diffusive traffic flow model. *Applied Mathematics in Science and Engineering*, 1-12.

[11] Fosu, G.O., & Oduro, F.T. (2020). Two-dimensional anisotropic macroscopic second-order traffic flow model. *Journal of Applied Mathematics and Computational Mechanics, 19*(2), 59-71.

[12] Lighthill, M.J., & Whitham, G.B. (1955). On kinematic waves II: A theory of traffic flow on long crowded roads. *Proc R Soc Lond A Math Phys Sci, 229*(1178), 317-345.
[13] Richards, P. I. (1956). Shock waves on the highway. *Operations research, 4*(1), 42-51.
[14] Payne, H. J. (1971). Model of freeway traffic and control. *Mathematical Model of Public System*, 51-61.
[15] Whitham, G.B. (1974). *Linear and Nonlinear Waves*. John Wiley and Sons, New York.
[16] K´uhne, R. (1984). Macroscopic freeway model for dense traffic-stop-start waves and incident detection. *Transportation and traffic theory, 9*, 21-42.
[17] Kerner, B. S., & Konh´a user, P. (1994). Structure and parameters of clusters in traffic flow. Physical Review E, 50(1), 54.
[18] Zhang, H. M. (1998). A theory of nonequilibrium traffic flow. *Transportation Research Part B: Methodological, 32*(7), 485-498.
[19] Helbing, D., & Johansson, A.F. (2009). On the controversy around Daganzo's requiem for and Aw-Rascle's resurrection of second-order traffic flow models. *Eur. Phys. J. B, 69*, 549-562.
[20] Daganzo, C.F. (1995). Requiem for second-order approximations of traffic flow. *Transp. Res. B: Methodol, 29*(4), 277-286.
[21] Heidemann, D. (1999). Some critical remarks on a class of traffic flow models. *Transp. Res. B: Methodol, 33*(2), 153-155.
[22] Treiber, M., Hennecke, A., & Helbing, D. (1999). Derivation, properties, and simulation of a gas-kinetic-based, nonlocal traffic model. *Physical Review E, 59*(1), 239-253.
[23] Aw, A. A. T. M., & Rascle, M. (2000). Resurrection of" second order" models of traffic flow. S*IAM journal on applied mathematics, 60*(3), 916-938.
[24] Rascle, M. (2002). An improved macroscopic model of traffic flow: derivation and links with the Lighthill-Whitham model. *Mathematical and computer modelling, 35*(5-6), 581-590.
[25] Zhang, H. M. (2002). A non-equilibrium traffic model devoid of gas-like behavior. *Transportation Research Part B: Methodological, 36*(3), 275-290.
[26] Jiang, R., Wu, Q. S., & Zhu, Z. J. (2002). A new continuum model for traffic flow and numerical tests. *Transportation Research Part B: Methodological, 36*(5), 405-419.
[27] Yu, L., Li, T., & Shi, Z. K. (2010). The effect of diffusion in a new viscous continuum traffic model. *Physics Letters A, 374*(23), 2346-2355.
[28] Zhang, H. M. (2009). Comment on "On the controversy around Daganzo's requiem for and Aw-Rascle's resurrection of second-order traffic flow models" by D. Helbing and AF Johansson: What faster-than-traffic characteristic speeds mean for vehicular traffic flow. *The European Physical Journal B, 69*, 563-568.
[29] Helbing, D. (2009). Reply to comment on "On the controversy around Daganzo's requiem for and Aw-Rascle's resurrection of second-order traffic flow models" by H. M. Zhang. *The European Physical Journal B, 69*, 569-570.
[30] Phillips, W. (1979). Kinetic model for traffic flow with continuum implications. *Transp. Plan. Technol*, *5*, 131-138.
[31] Papageogiou, M., Blosseville, J.M., & Hadj-Salem, H. (1989). Macroscopic modeling of traffic flow on the boulevard peripherique in Paris. *Transp. Res. B: Methodol, 23*, 29-47.
[32] Chandler, R., Herman, R., & Montroll, E. (1958). Traffic dynamics: Studies in car following. *Oper. Res, 6(2), 165-184.*
[33] Rosas-Jaimes, O.A., Luckie-Aguirre, O., & Rivera, J.C.L. (2013). Sensitivity Parameter of a Microscopic Traffic Model. In *Congreso Nacional de Control Automatico, Ensenada, Baja California, Mexico*.
[34] Helbing, D., & Schreckenberg, M. (1999). Cellular automata simulating experimental properties of traffic flow. *Phys. Rev. E, 59(3).*
[35] Helbing, D., & Vicsek, T. (1999). Optimal self-organization. *New J. Phys, 1(13), 1-17.*
[36] Caligaris, C., Sacone, S.,& Siri, S. (2010). On the Payne-Whitham differential model stability constraints in one-class and two-class cases. *Appl. Math. Sci, (76)*, 3795-3821.
[37] Ferrara, A., Sacone, S., & Siri, S. (2018). *Freeway Traffic Modelling and Control*. Springer.
[38] Del Castillo, J.M., & Benitez, F.G. (1995). On functional form of the speed-density relationship - I: general theory, II: empirical investigation. *Transp. Res. B: Methodol, (29)*, 373-406.